chemistry

MDPI

Article

Fractionation of Lignocellulose in a Pressurized Ammonia Mixed Solvent System

Yan Li *, Yuxuan Han, Bo Wang, Shuang Ding, Xu Zeng, Yalan Yan, Bo Ren * and Xiaodong Yang *

Jilin Provincial Key Laboratory of Straw-Based Functional Materials, Institute for Interdisciplinary Biomass Functional Materials Studies, Jilin Engineering Normal University, Changchun 130052, China; 15835292208@163.com (Y.H.); wangbo0306@jlenu.edu.cn (B.W.); dingshuang2018@163.com (S.D.); zengxu15@jlenu.edu.cn (X.Z.); yanyalan15@163.com (Y.Y.)

* Correspondence: yanlicc0206@163.com (Y.L.); renbo1000@126.com (B.R.); y86908051@126.com (X.Y.)

Abstract

Lignocellulose represents an abundant and renewable biomass feedstock; however, its intrinsically recalcitrant cross-linked network of cellulose, hemicellulose, and lignin poses a significant barrier to the efficient fractionation and high-value utilization of its individual components. In response to this challenge, this study established a pressurized ammonia–solvent system for lignocellulosic component separation. Single-factor exploratory experiments were performed to probe general trends of key operational parameters including reaction temperature, system pressure, and solvent composition. Among the tested ranges, the preferable conditions were identified as follows: 50 vol% ethanol aqueous solution, a reaction temperature of 200 °C, a holding time of 6 h, and an ammonia pressure of 8 MPa. Under these selected operating parameters, the cellulose purity in the cellulose-enriched fraction reached 89.6 ± 1.4% with a cellulose recovery of 85.0 ± 2.1%. Microstructural and crystalline variations, characterized by SEM and XRD, confirmed that the combined solvent system effectively disrupted the fibrous structure and native cellulose crystalline arrangement of raw biomass. Elemental analysis and XPS characterization further verified that ammonia-derived nitrogen species were preferentially incorporated into lignin-enriched fractions, occurring in both covalently bonded and adsorbed forms, while negligible nitrogen was detected in cellulose- and hemicellulose- enriched fractions. This work explores pressurized ammonia-assisted fractionation to achieve selective component separation of agricultural straw biomass and offers an approach toward graded utilization of lignocellulosic resources.

Keywords: lignocellulose; fractionation; ammonia; solvent; pressurized system

Check for updates

Academic Editor: Oliver Kröcher

Received: 3 August 2026
Revised: 24 September 2026
Accepted: 28 September 2026
Published: 29 September 2026

Copyright: © 2026 by the authors. Licensee MDPI, Basel, Switzerland. This article is an open access article distributed under the terms and conditions of the Creative Commons Attribution (CC BY) license.

1. Introduction

Lignocellulosic biomass, sourced from agricultural straw residues, forestry waste, and industrial organic by-products, supplemented by dedicated energy crops, represents the most abundant renewable organic carbon feedstock on Earth [1–3]. It exhibits immense potential to replace fossil resources for manufacturing biofuels, chemicals and functional materials [2,4]. However, the inherent recalcitrance of lignocellulose, arising from its complex cross-linked network of cellulose, hemicellulose, and lignin, severely restricts its efficient fractionation and downstream valorization. Cellulose, a crystalline polymer of glucose, is tightly enmeshed with hemicellulose and further encapsulated by a hydrophobic lignin matrix, forming a physicochemical barrier that impedes enzymatic hydrolysis and

chemical conversion of biomass [5,6]. Consequently, the selective deconstruction of this intricate architecture while preserving the structural integrity of individual components remains a central challenge in lignocellulosic biorefining.

To overcome the inherent structural recalcitrance of lignocellulosic biomass, various pretreatment and fractionation technologies, including physical [7–9], chemical [10–14], biological [15,16] and physicochemical/biochemical combined methods [17–22], have been developed for efficient biomass utilization. Conventional physical treatments such as mechanical crushing and ultrasonic vibration only disrupt the macroscopic fibrous structure of raw materials, failing to achieve effective component separation and lignin removal. Biological pretreatment is environmentally friendly and operates under mild conditions, but its practical application is limited by long treatment duration, low processing efficiency and poor scalability. Common chemical approaches, including dilute acid, dilute alkali and organic solvent pretreatment, can effectively disrupt the compact lignocellulosic network. However, these methods usually cause severe degradation of cellulose and hemicellulose, generate a large number of fermentation inhibitors, and cannot realize collaborative high-value utilization of all biomass components.

Among various chemical pretreatment technologies, alkaline pretreatment, especially ammonia-based treatment, has gained widespread research attention due to its favorable delignification performance [23,24]. Typical ammonia-based technologies, such as ammonia fiber expansion (AFEX) and soaking in aqueous ammonia (SAA), can selectively cleave ester and ether bonds in lignin-carbohydrate complexes (LCCs), break the inherent recalcitrant structure of biomass, and improve the enzymatic digestibility of cellulose. Nevertheless, these two mature technologies have unavoidable technical limitations. AFEX mainly relies on physical explosion to loosen biomass structure, which only induces lignin redistribution rather than efficient dissolution and removal, resulting in poor pretreatment performance for high-lignin biomass. SAA can effectively dissolve lignin, but a long reaction time or elevated temperature easily triggers polysaccharide peeling reactions and causes severe loss of hemicellulosic sugars. In general, conventional ammonia pretreatment has a narrow feasible process window. Strict reaction conditions for high delignification efficiency will inevitably degrade hemicellulose, while mild conditions for sugar preservation cannot fully disrupt the stable LCC cross-linked structure. This technical bottleneck restricts the efficient and high-value fractionation of lignocellulose, highlighting the necessity of developing selective pretreatment technologies that can precisely deconstruct lignocellulosic structure, maintain cellulose integrity, and realize synchronous recovery of hemicellulose and lignin.

Fluid-based pretreatment technologies have been widely adopted for lignocellulosic fractionation due to their favorable mass transfer and extraction properties, which reduce solvent consumption and waste generation relative to traditional pretreatment approaches [25–27]. However, most conventional fluid pretreatment relies on rigorous supercritical or subcritical conditions that demand high-standard pressure-resistant equipment and high operational costs, thereby limiting their applicability. As a viable alternative, pressurized ammonia pretreatment can enhance the alkalinity and nucleophilic reactivity of ammonia under pressure, which disrupts the cross-linked lignocellulosic network and partially breaks lignin–carbohydrate complex linkages; additionally, ammonia can be recovered through vacuum vaporization for reuse, supporting its recyclable potential for biomass processing. Nevertheless, single pressurized ammonia systems still exhibit limitations in component selectivity and structural regulation efficiency. Although ammonia-based pretreatment has been well validated in previous studies [28,29], most investigations merely focus on pure ammonia systems, while fractionation performance and component-response mechanisms under pressurized ammonia–organic mixed solvent conditions remain insufficiently explored. Specifically, the divergent structural eVolu-

tion behaviors of cellulose, hemicellulose, and lignin during mixed solvent pressurized pretreatment are still poorly understood, restricting the further development of targeted lignocellulose fractionation strategies.

This study developed a novel pressurized ammonia mixed solvent system for the fractionation of lignocellulosic biomass. The effects of key operational parameters, including reaction temperature, system pressure, and solvent composition, on biomass fractionation performance were investigated through single-factor experiments, and the preferable pretreatment conditions were determined. The structural and physicochemical variations in lignocellulose before and after pretreatment were characterized via scanning electron microscopy (SEM), X-ray diffraction (XRD), X-ray photoelectron spectroscopy (XPS) and elemental analysis. Moreover, the selective nitrogen doping behavior of ammonia on different biomass components was explored and clarified. This work explores a feasible fractionation strategy for the graded separation of lignocellulosic components and provides fundamental insights and technical references for the comprehensive utilization of agricultural straw resources and the development of biorefinery technologies.

2. Materials and Methods

2.1. Materials

Corn straw was collected from the surrounding areas of Changchun, Jilin Province, China, in October 2024. NH_3 was supplied by Dalian Special Gases (99.9 wt%, Dalian, China). Toluene (PhMe), anhydrous ethanol (EtOH), concentrated sulfuric acid, tert-butanol (t-BuOH), iso-butanol (i-BuOH), and γ-valerolactone (GVL) were purchased from Sinopharm Chemical Reagent Co., Ltd. (Shanghai, China). Deionized water was laboratory-prepared. All chemical reagents were used as received except concentrated sulfuric acid, which was diluted prior to use.

2.2. Removal of Extractives

First, the corn straw was crushed with a pulverizer (Bear Electric Appliance Co., Ltd., Foshan, China) and sieved through a 40-mesh sieve, followed by drying at 50 °C for 6 h, and then packed into self-made gauze bags. Subsequently, sequential Soxhlet extraction was performed on the corn straw. The sample was first refluxed with 300 mL of water for 12 h to remove water-soluble impurities, followed by 300 mL of toluene–ethanol mixture (2:1, v/v) under reflux for another 12 h to extract organic components including tannins, lipids, resins, and waxes. After extraction, the treated corn straw was washed three times with 30 mL of anhydrous ethanol to eliminate residual extractives, air-dried in a fume hood, and finally dried in a vacuum drying oven at 50 °C for 6 h. The dried corn straw lignocellulose was crushed and sieved through a 40-mesh screen. The milled samples were sealed in polyethylene bags and stored in a desiccator at room temperature before use.

2.3. Fractionation of Lignocellulose in Pressurized Ammonia Mixed Solvent System

A certain mass of the dried corn straw lignocellulose (0.1, 0.2, 0.4, and 0.8 g) together with 20 mL of solvent (water, tert-butanol, toluene, γ-valerolactone, etc.) was loaded into a 100 mL high-pressure autoclave (Jiangsu Tuochuang Scientific Research Instrument Co., Ltd., Hai'an, China). After sealing, the reactor was purged with pure nitrogen three times to remove residual air. The autoclave was preheated in an oil bath to the preset reaction temperature (180, 200, 220, and 240 °C) for 10 min, and liquid ammonia was subsequently introduced into the reactor using an ammonia pump (Depamu (Hangzhou) Pumps Technology Co., Ltd., Hangzhou, China) until the target pressure (2–28 MPa) was reached. The high-pressure autoclave was equipped with a Grade 1.6 Bourdon tube pressure gauge (0–40 MPa, Jiangsu Tuochuang Scientific Research Instrument Co., Ltd.,

Hai'an, China) for on-site visual pressure indication. The high-pressure autoclave has a maximum allowable working pressure of 35 MPa at 250 °C. Owing to the gas–liquid two-phase equilibrium of ammonia under pressurized conditions, its exact mass or molar amount could not be determined by simple gravimetric measurements. Therefore, the ammonia loading was indirectly controlled by adjusting the system pressure to preset target values. It should be noted that the so-called "pressure effect" in this study does not represent the influence of pressure alone, but rather a combined effect of the equilibrium pressure and the corresponding ammonia loading. The reaction timer was started once stirring was initiated at a rotation speed of 1200 r/min, and the reaction was maintained for a designated duration ranging from 2 to 8 h. Upon completion of the reaction, stirring was stopped, and the autoclave was cooled to room temperature in a water bath. Ammonia gas was then slowly vented and absorbed by deionized water.

After the reaction, the reaction mixture was filtered to separately collect the filter residue and filtrate. Both fractions were dialyzed against deionized water with a dialysis membrane (MWCO = 100 Da) for 2 days with three water changes (approximately 5 L deionized water for each exchange) until the dialysate reached neutral pH, followed by freeze-drying. The membrane retained most organic components; only trace impurities with molecular weights below 100 Da (e.g., inorganic salts, low-molecular-weight organic acids and residual ammonia) were removed, while sugars and oligosaccharides were preserved in the retentate. The freeze-dried filter residue was designated as Solid I, which was cellulose-enriched, whereas Solid II (hemicellulose- and lignin-enriched) was obtained from the dialyzed and freeze-dried filtrate. Solid II was further treated by acetone extraction to produce a lignin-rich acetone extract and Solid Residue III (hemicellulose-enriched acetone-insoluble fraction). The detailed fractionation procedure is illustrated in Figure 1.

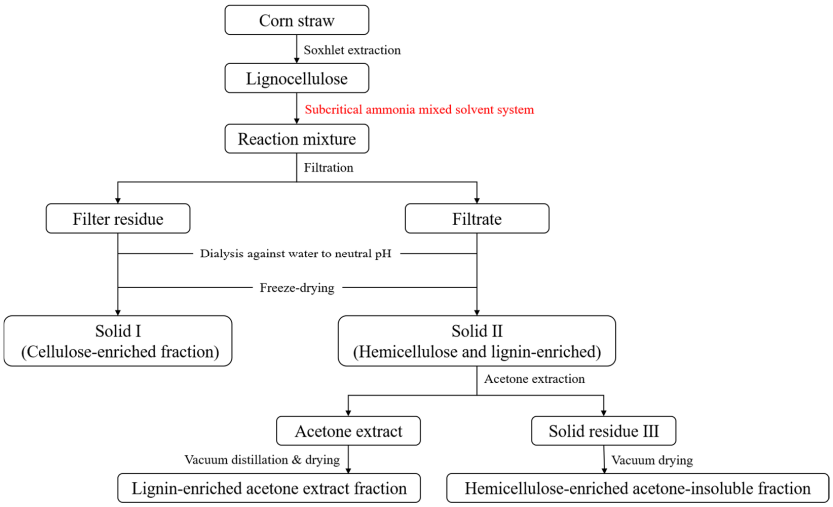


Figure 1. Schematic diagram for the fractionation of corn straw-derived lignocellulose in a pressurized ammonia mixed solvent system.

All experiments were conducted using a single batch of lignocellulose to eliminate feedstock variability as a potential source of experimental scatter. Prior to the systematic single-factor experiments, the reproducibility of the high-pressure batch reactor system was verified through three independent replicate experiments under representative conditions (180 °C, 15 MPa, water, 4 h). The relative standard deviation (RSD) of the product yield was less than 5%, confirming satisfactory experimental repeatability. Therefore, single measurements were adopted for the subsequent screening experiments to balance data reliability with experimental feasibility. The weight percentage of product, cellulose purity, and cellulose recovery were calculated as follows:

$$Weight\ percentage\ of\ product\ (\%) = \frac{M\ product}{M\ corn\ straw-derived\ lignocellulose} \times 100\%$$

$$Cellulose\ purity\ (\%) = \frac{M\ cellulose}{M\ cellulose-enriched\ fraction} \times 100\%$$

$$Cellulose\ recovery\ (\%) = \frac{M\ cellulose}{M\ cellulose\ in\ dried\ corn\ straw\ lignocellulose} \times 100\%$$

where the product refers to the cellulose-enriched fraction, hemicellulose-enriched acetone-insoluble fraction or lignin-enriched acetone extract fraction obtained after separation.

2.4. Analysis of the Fractionated Components

2.4.1. Compositional Analysis of Corn Straw-Derived Lignocellulose and Cellulose-Enriched Solid

The chemical compositions of corn straw-derived lignocellulose and cellulose-enriched solid were determined in accordance with the standard NREL acid hydrolysis method [30]. The main components consist of cellulose, hemicellulose, and lignin, along with minor amounts of extractives and ash. Briefly, the solid was charged into 72% sulfuric acid at 30 °C for 60 min, followed by hydrolysis in 4% sulfuric acid at 120 °C for another 60 min.

Monomeric sugars such as glucose, xylose, and arabinose were assayed quantitatively using high-performance liquid chromatography (HPLC) with a refractive index detector (RID) and an Aminex HPX-87H column (300 × 7.8 mm, 9 µm, Bio-Rad, Hercules, CA, USA) at 60 °C; 5 mm sulfuric acid at 0.5 mL/min was used as the mobile phase. All carbohydrate standards, including glucose, xylose, arabinose, mannose, and galactose (purity ≥ 99.5%, Sigma-Aldrich, Saint Louis, MO, USA), were used for external calibration. A series of gradient standard solutions (1, 3, 6, 10, 15 g/L) were prepared to establish linear calibration curves, and good linearity was achieved over the applied concentration range $R^2 > 0.999$). Analytical recovery factors of 0.92, 0.88, and 0.89 were obtained for glucose, xylose, and arabinose, respectively.

Following that, a UV spectrophotometer (Hitachi High-Tech Science Corporation, Tokyo, Japan) was used to determine acid-soluble lignin (ASL) at 205 nm. Acid-insoluble Klason lignin was quantified by the gravimetric method. The ash content was measured by calcination at 575 °C.

2.4.2. Surface Morphology of Cellulose-Enriched Solid

The surface morphology of cellulose-enriched solid was characterized by scanning electron microscopy (SEM) using a Zeiss Gemini SEM 300 instrument (Zeiss, Oberkochen, Germany). Prior to observation, the dried samples were sputter-coated with a thin gold layer to improve electrical conductivity and mitigate charge accumulation. SEM images were acquired at an accelerating voltage of 3.00 kV using the SE2 detector (Carl Zeiss Microscopy GmbH, Jena, Germany). The working distance was set in the range of 5.5–9.4 mm for all samples. All micrographs were captured at a magnification of 1.00 K×. The aperture size was 30.00 µm, and the scale bar represented 10 µm. For each sample, at least 3 independent regions were randomly selected and observed at different magnifications to ensure the representativeness of the morphology. The images shown are typical representatives.

2.4.3. X-Ray Diffraction of Cellulose-Enriched Solid

The crystalline structure changes in raw and pretreated biomass samples were analyzed using an X-ray diffractometer (XRD, Rigaku SmartLab, Tokyo, Japan) with Cu Kα radiation (λ = 1.5406 Å) operating at 40 kV and 40 mA. All solid samples were uniformly ground and sieved through a 100-mesh screen and eVenly flattened on a glass sample holder to eliminate texture effects. The XRD patterns were collected over a 2θ scanning

range from 5° to 80°, with a step size of 0.01° and a scanning speed of 10°/min at room temperature and atmospheric conditions. No baseline smoothing or artificial peak fitting was performed to ensure the authenticity of spectral information.

2.4.4. Elemental Analysis of the Fractionated Components

Elemental analysis was performed using an Elementar Vario EL elemental analyzer (Elementar Analysensysteme GmbH, Langenselbold, Germany) to quantify the nitrogen content of fractionated biomass components.

2.4.5. X-Ray Photoelectron Spectroscopy of Lignin-Enriched Acetone Extract Fraction

X-ray photoelectron spectroscopy (XPS) was performed on a Thermo Scientific K-Alpha spectrometer (Thermo Fisher Scientific, Inc., Waltham, MA, USA) equipped with an Al Kα monochromatic X-ray source (1486.6 eV, Thermo Fisher Scientific, Inc., Waltham, MA, USA). Survey spectra and high-resolution N 1s spectra were acquired at pass energies of 100 eV and 20 eV, respectively. The binding energy scale was calibrated against the adventitious carbon C 1s peak at 284.8 eV. Shirley background subtraction and Gaussian–Lorentzian (GL) peak deconvolution were carried out using CasaXPS software (version 2.3.26, Casa Software Ltd., Teignmouth, UK). The full width at half maximum (FWHM) of component peaks was constrained below 1.8 eV to avoid artificial overfitting.

3. Results and Discussion

3.1. Chemical Composition of the Dried Corn Straw Lignocellulose

The components of corn straw lignocellulose were determined according to the standard analytical procedure established by the National Renewable Energy Laboratory (NREL) of the United States. The mass fractions of cellulose, hemicellulose, acid-insoluble lignin, acid-soluble lignin, ash, and moisture content are summarized in Table 1.

Table 1. Chemical composition of corn straw lignocellulose.

No.	Composition	Mass Fraction (%)
1	Cellulose	45.6 ± 0.6
2	Hemicellulose	25.9 ± 0.4
3	Acid-insoluble lignin	16.7 ± 0.3
4	Acid-soluble lignin	2.7 ± 0.1
5	Ash	1.6 ± 0.2
6	Moisture content	1.2 ± 0.4

3.2. Preliminary Optimization of Lignocellulose Fractionation in Pressurized Ammonia Mixed Solvent System

3.2.1. Effect of Reaction Temperature on Lignocellulose Fractionation

A total of 0.4 g of pretreated corn straw lignocellulose was mixed with 20 mL of deionized water, and hydrothermal fractionation was performed at 180, 200, 220, and 240 °C for 4 h under a constant system pressure of 15 MPa. As illustrated in Figure 2, within this temperature range, the reaction temperature exerted a modest effect on the relative contents of the cellulose-enriched fraction, hemicellulose-enriched acetone-insoluble fraction, and lignin-enriched acetone extract fraction after fractionation. Notably, at 180 °C, cellulose only accounted for 65.9% of the cellulose-enriched fraction. The proportion of cellulose gradually increased with rising temperature and reached a maximum of 82.8% at 200 °C. When the temperature exceeded 200 °C, the cellulose purity remained above 80%. Nevertheless, further elevation of temperature induced slight thermal degradation of cellulose and decreased its relative proportion. Taking all factors into consideration, 200 °C was selected as the preferable reaction temperature.

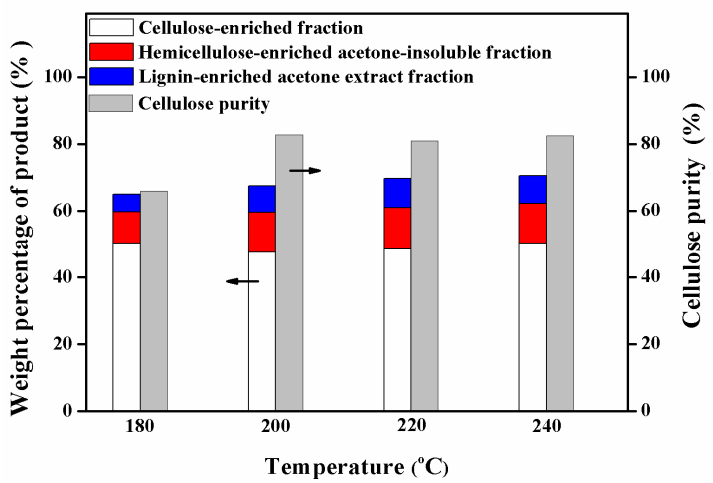


Figure 2. Effects of temperature on fractionation of lignocellulose in pressurized ammonia mixed solvent system. Reaction conditions: 0.4 g pretreated corn straw lignocellulose, 20 mL deionized water, 15 MPa, 4 h. Single measurement was performed for each screening condition. System reproducibility was pre-validated via triplicate tests under representative reaction conditions, with RSD < 5%. The left-pointing arrows correspond to the left vertical axis, and the right-pointing arrows correspond to the right vertical axis. Raw data are provided in the Supplementary Information.

3.2.2. Effect of Reaction Time on Lignocellulose Fractionation

With the preferable reaction temperature of 200 °C and system pressure fixed at 15 MPa, 0.4 g of pretreated corn straw lignocellulose was dispersed in 20 mL of deionized water. The hydrothermal fractionation reactions were performed for 2, 4, 6, and 8 h to investigate the effect of reaction duration on the fractionation of lignocellulose, and the results are presented in Figure 3. The reaction time exerted a modest influence on the relative contents of the cellulose-enriched fraction, hemicellulose-enriched acetone-insoluble fraction, and lignin-enriched acetone extract fraction after fractionation. However, when the reaction time was 2 h, the relative cellulose purity in the cellulose-enriched fraction was only 70.3%. The prolonged reaction duration promoted the continuous removal of hemicellulose and lignin, thereby gradually increasing the cellulose proportion, which reached a maximum of 84.2% at 6 h. Nevertheless, further extending the reaction time to 8 h caused slight thermal degradation and side reactions of cellulose under prolonged hydrothermal conditions, reducing the relative cellulose purity to 79.6%. Considering the comprehensive enrichment efficiency and structural stability of cellulose, 6 h was determined as the preferable reaction time.

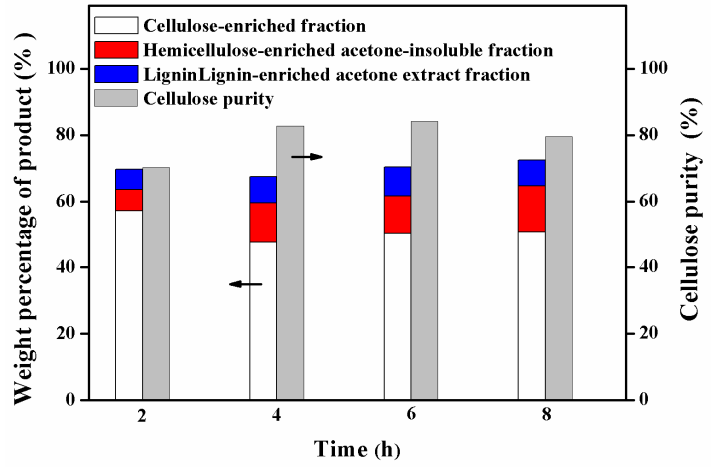


Figure 3. Effect of reaction time on fractionation of lignocellulose in pressurized ammonia mixed solvent system. Reaction conditions: 0.4 g pretreated corn straw lignocellulose, 20 mL deionized water,

15 MPa, 200 °C. Single measurement was performed for each screening condition. System reproducibility was pre-validated via triplicate tests under representative reaction conditions, with RSD < 5%. The left-pointing arrows correspond to the left vertical axis, and the right-pointing arrows correspond to the right vertical axis. Raw data are provided in the Supplementary Information.

3.2.3. Effect of Substrate Loading on Lignocellulose Fractionation

With the preferable reaction conditions of 200 °C, 6 h and a constant system pressure of 15 MPa, 0.1 g, 0.2 g, 0.4 g, and 0.8 g of pretreated corn straw lignocellulose were separately added into 20 mL of deionized water to explore the effect of substrate loading on the fractionation of lignocellulose. The experimental results are shown in Figure 4. The substrate loading exerted a mild influence on the relative contents of the cellulose-enriched fraction, hemicellulose-enriched acetone-insoluble fraction and lignin-enriched acetone extract fraction after fractionation. Notably, the relative cellulose purity in the cellulose-enriched fraction remained above 80% under all dosage conditions, achieving a stable and efficient cellulose enrichment effect. Considering the raw material utilization efficiency, reaction system adaptability and experimental economy comprehensively, 0.4 g was selected as the preferable substrate loading.

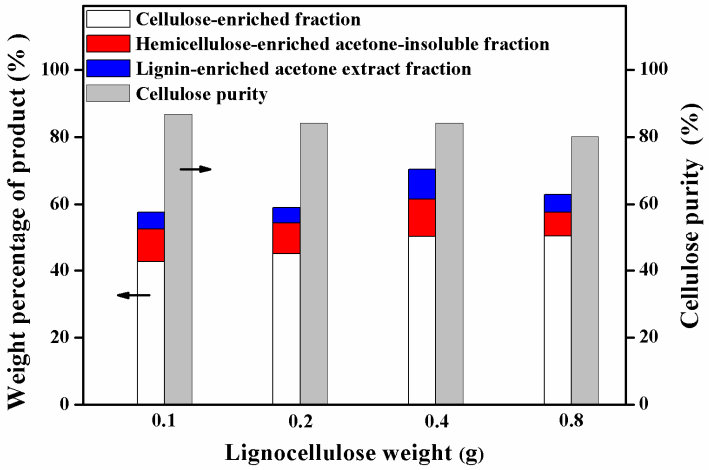


Figure 4. Effect of substrate loading on fractionation of lignocellulose in pressurized ammonia mixed solvent system. Reaction conditions: 20 mL deionized water, 15 MPa, 200 °C, 6 h. Single measurement was performed for each screening condition. System reproducibility was pre-validated via triplicate tests under representative reaction conditions, with RSD < 5%. The left-pointing arrows correspond to the left vertical axis, and the right-pointing arrows correspond to the right vertical axis. Raw data are provided in the Supplementary Information.

3.2.4. Effect of Reaction Pressure on Lignocellulose Fractionation

Under the fixed preferable conditions (0.4 g corn straw lignocellulose, 20 mL deionized water, reaction temperature of 200 °C, and reaction duration of 6 h), experiments were conducted at system pressures of 2, 3, 8, 12, 15, and 28 MPa to investigate the pressure-regulated lignocellulose fractionation performance of the pressurized ammonia–water mixed solvent system. The corresponding results are presented in Figure 5. Notably, the variations in lignocellulose fractionation efficiency do not originate from the independent effect of pressure alone. Instead, they are governed by the coupled effects of system pressure, ammonia solubility in the aqueous phase, and water-dependent ammonia partitioning behavior.

System pressure showed a modest influence on the relative contents of the cellulose-enriched fraction, hemicellulose-enriched acetone-insoluble fraction, and lignin-enriched acetone extract fraction after fractionation. However, pressure exerted a pronounced influence on the cellulose purity of the cellulose-enriched fraction. At a low pressure of

2 MPa, limited ammonia solubility in water leads to a low dissolved ammonia concentration and weakened fractionation effect, resulting in a low cellulose purity of only 62.1% in the cellulose-enriched fraction. With the elevation of system pressure, the rise in ammonia solubility in the aqueous phase increases the concentration of dissolved reactive ammonia, which significantly improves lignocellulose fractionation and leads to a steady increase in cellulose purity. When the pressure reached 8 MPa, the pressurized ammonia–water system achieved a stable reaction state with adequate dissolved ammonia, and the cellulose purity was greatly improved to 82.5%. Further increasing the pressure to 12 MPa and 15 MPa only slightly increased the cellulose purity to 84.5% and 84.2%, respectively, with no remarkable enhancement in fractionation performance compared with the 8 MPa condition, because ammonia solubility in water gradually approaches saturation. Excessively high pressure (28 MPa) destroyed the stable coupled reaction environment of the ammonia-water system and may induce slight cellulose degradation, which decreased the cellulose purity to 78.6%. Comprehensive consideration of cellulose enrichment efficiency, energy consumption, and operational safety confirms that 8 MPa is the preferable reaction pressure for the pressurized ammonia–water mixed solvent fractionation system.

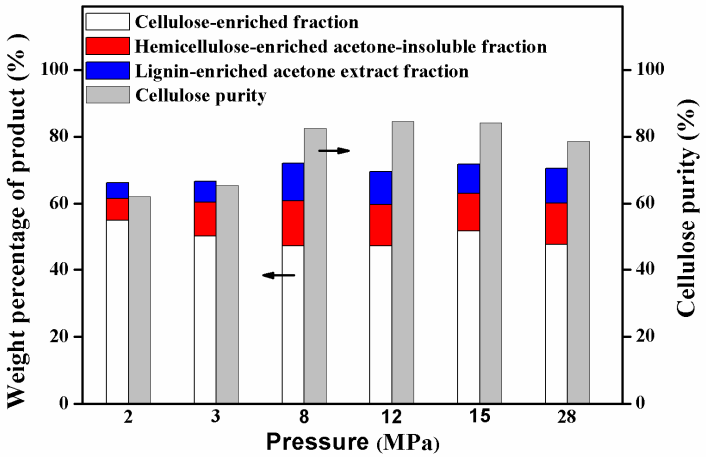


Figure 5. Effect of reaction pressure on fractionation of lignocellulose in pressurized ammonia mixed solvent system. Reaction conditions: 0.4 g pretreated corn straw lignocellulose, 20 mL deionized water, 200 °C, 6 h. Single measurement was performed for each screening condition. System reproducibility was pre-validated via triplicate tests under representative reaction conditions, with RSD < 5%. The left-pointing arrows correspond to the left vertical axis, and the right-pointing arrows correspond to the right vertical axis. Raw data are provided in the Supplementary Information.

3.2.5. Effect of Solvent on Lignocellulose Fractionation

With the preferable process parameters (0.4 g lignocellulose dosage, reaction temperature of 200 °C, reaction time of 6 h, and system pressure of 8 MPa), seven different solvents including deionized water, ethanol, tert-butanol, iso-butanol, toluene, γ-valerolactone (GVL), and 50 vol% ethanol aqueous solution were adopted with a constant solvent volume of 20 mL to explore the effects of solvent types on the lignocellulose fractionation in the pressurized ammonia system. The corresponding results are illustrated in Figure 6. The solvent type substantially affects the fractionation performance, primarily because solvent polarity determines the solvation energy, solubility, and reactive state of ammonia, thereby regulating the deconstruction of lignocellulosic networks. Distinct differences in the relative contents of cellulose-enriched solids, hemicellulose-rich acetone-insoluble fractions, and lignin-enriched acetone extracts, as well as significant variations in cellulose purity and recovery, were observed across different solvent media.

Notably, the nonpolar solvent toluene exhibits extremely low ammonia solvation capacity, leading to insufficient activation and dispersion of ammonia. Accordingly, it

delivered the poorest fractionation performance, with a cellulose purity of only 42.6% and a moderate cellulose recovery of 72.4%. In contrast, high-polarity deionized water and pure ethanol possess favorable ammonia solvation energy, enabling effective ammonia dissolution and activation. These two polar media achieved satisfactory cellulose enrichment, with cellulose purities of 82.5% and 78.9% and cellulose recoveries of 86.8% and 78.0%, respectively. Weakly polar GVL, tert-butanol, and iso-butanol display mismatched solvation energy for ammonia, which restricts the formation of active ammonia species and weakens biomass deconstruction. Consequently, these solvents yielded inferior fractionation efficiency, with low cellulose purities of 50.6%, 40.2%, and 35.9% and corresponding cellulose recoveries of 69.3%, 72.7%, and 65.4%. In particular, the bulky molecular structure and steric hindrance of tert-butanol and iso-butanol further limit solvent penetration into the compact lignocellulosic matrix, resulting in the lowest cellulose purity despite their relatively acceptable cellulose retention.

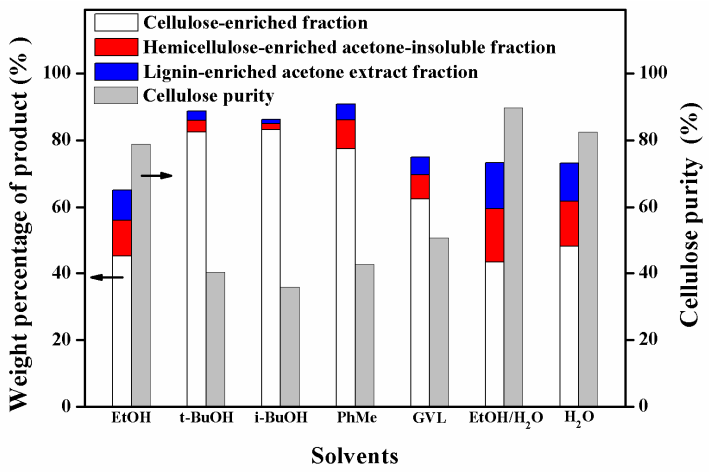


Figure 6. Effects of different solvents on fractionation of lignocellulose in pressurized ammonia mixed solvent system. Reaction conditions: 0.4 g pretreated corn straw lignocellulose, 20 mL solvent, 200 °C, 8 MPa, 6 h. Single measurement was performed for each screening condition. System reproducibility was pre-validated via triplicate tests under representative reaction conditions, with RSD < 5%. The left-pointing arrows correspond to the left vertical axis, and the right-pointing arrows correspond to the right vertical axis. Raw data are provided in the Supplementary Information.

Consistent with the common trade-off between cellulose purity and recovery in lignocellulose biorefining, single solvents generally fail to achieve dual optimization of the two indicators, which is closely associated with their inherent ammonia solvation characteristics. High-polarity water provides excellent ammonia solvation and activation, thus maximizing cellulose recovery (86.8%), yet it cannot completely eliminate non-cellulosic components, resulting in limited cellulose purity. Weakly polar organic solvents show poor ammonia solvation ability, which restricts impurity removal efficiency, ultimately leading to low cellulose purity and unsatisfactory comprehensive fractionation performance.

In comparison, the 50 vol% ethanol aqueous binary system presents optimized ammonia solvation energy and balanced solvent polarity and permeability. This binary medium can moderately stabilize and activate dissolved ammonia species, facilitating effective lignin dissolution and disruption of lignin–carbohydrate cross-linked structures to expose cellulose skeletons and improve solid purity. Meanwhile, the binary solvent environment may regulate hydrogen bond disruption within cellulose microcrystals and moderates structural relaxation, avoiding excessive cellulose degradation. Benefiting from the optimized ammonia solvation behavior and complementary solvent properties, the ethanol–water binary system achieved the best comprehensive fractionation performance, with a maximum

cellulose purity of 89.6 ± 1.4% and a favorable cellulose recovery of 85.0 ± 2.1%, realizing a well-balanced cellulose purification and retention effect.

Under the preferable conditions (50 vol% ethanol aqueous solution system), the total recovered solid yield was 73.4 ± 1.5%, of which the cellulose-enriched fraction accounted for 43.3 ± 1.1%, the hemicellulose-enriched acetone-insoluble fraction for 16.3 ± 0.7%, and the lignin-enriched acetone extract fraction for 13.8 ± 0.4%. The overall mass loss during fractionation arises from both chemical degradation and physical material losses. Under pressurized alkaline ammonia conditions, dissolved hemicellulosic pentoses undergo successive alkaline degradation to produce low-molecular-weight organic acids (e.g., formic and acetic acids), which are removed via dialysate and excluded from subsequent fractionation. Meanwhile, deconstruction of pretreated biomass generates abundant ultrafine particles; some ultrafine cellulose and lignin microparticles penetrate filter membranes during repeated filtration and cannot be recovered into the cellulose-rich fraction. In addition, material adhesion on the inner surfaces of reactors, filtration units, dialysis devices and extraction vessels during multi-step transfers further contributes to mass loss, collectively leading to the observed total solid recovery below 100%.

Based on the above single-factor exploratory experimental results, the preferable process conditions for the fractionation of corn straw lignocellulose in the pressurized ammonia mixed solvent system were determined as follows: a lignocellulose dosage of 0.4 g, 20 mL of 50 vol% ethanol aqueous solution as the solvent, a reaction temperature of 200 °C, a reaction time of 6 h, and a constant system pressure of 8 MPa. Under the preferable conditions, the cross-linked structure of lignocellulose may be efficiently disrupted, hemicellulose and lignin can be effectively removed, and the relative purity of cellulose in the cellulose-enriched fraction can be significantly improved. These conditions enable favorable performance in the selective fractionation of lignocellulose and high-purity cellulose enrichment.

3.3. Analysis of Lignocellulose Fractionation Products in Pressurized Ammonia Mixed Solvent System

3.3.1. SEM Analysis

Figure 7 displays the SEM morphologies of raw lignocellulose and the cellulose-enriched fraction in different solvent systems. The raw corn straw lignocellulose presents a smooth and intact surface, where the fibrous structure is tightly wrapped with no exposed cellulose skeleton, showing a regular and stable structural morphology. After treatment with the non-polar solvent toluene and weak-polar solvent tert-butanol, the lignocellulose fibers maintain a relatively complete structure with slight surface damage and limited local fragmentation, indicating a weak structural destruction effect. In contrast, lignocellulose treated with strong polar solvents (water and ethanol) exhibits obvious surface cracks and defects. The rigid cross-linked structure formed by lignin and hemicellulose is effectively disrupted, and the dissolution of hemicellulose and lignin generates uneven sheet-like structures and porous morphologies on the fiber surface. Notably, lignocellulose treated with 50 vol% ethanol aqueous solution shows the most severe structural damage. The surface layers of fibers are largely stripped, the internal cellulose skeleton is fully exposed, and the degree of surface fragmentation and fuzzing increases significantly. The observed differences in fiber structural damage can indirectly support the regulatory effect of solvent polarity on lignocellulose fractionation. Combined with the above component variation results, it is speculated that the ethanol–water composite solvent can efficiently disrupt the cross-linked network of lignocellulose, facilitate the removal of hemicellulose and lignin, and thereby contribute to the efficient enrichment of cellulose.

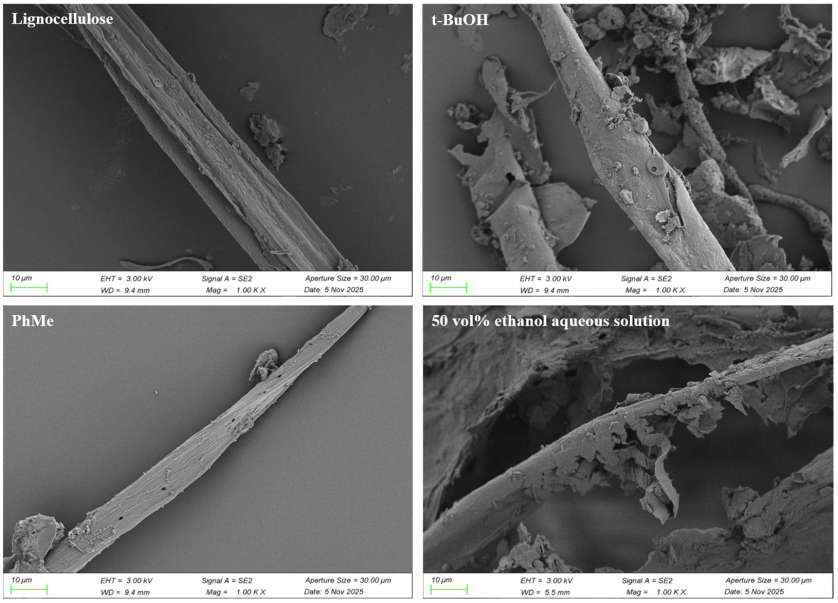


Figure 7. SEM analysis of lignocellulose and the cellulose-enriched fraction in different solvents.

3.3.2. XRD Analysis

Figure 8 presents the XRD patterns of raw lignocellulose and cellulose-enriched fractions from different solvent systems. For raw lignocellulose, characteristic diffraction peaks were observed at 2θ of 15.0°, 16.4°, 22.5°, and 34.5°, which correspond to the typical cellulose I crystal structure. Notably, the characteristic crystal planes of cellulose II are generally located at approximately 13.0°, 20.0°, and 22.0° [31,32]. Since the dominant diffraction peaks of the tested samples were concentrated near 22.5°, this may suggest that cellulose I remained the predominant crystal configuration. Except for the group treated with 50 vol% ethanol aqueous solution, raw lignocellulose and the cellulose-enriched fraction obtained from other solvent systems exhibited relatively strong diffraction peaks ranging from 16.5° to 22.5°, implying that the cellulose I crystal structure was largely retained.

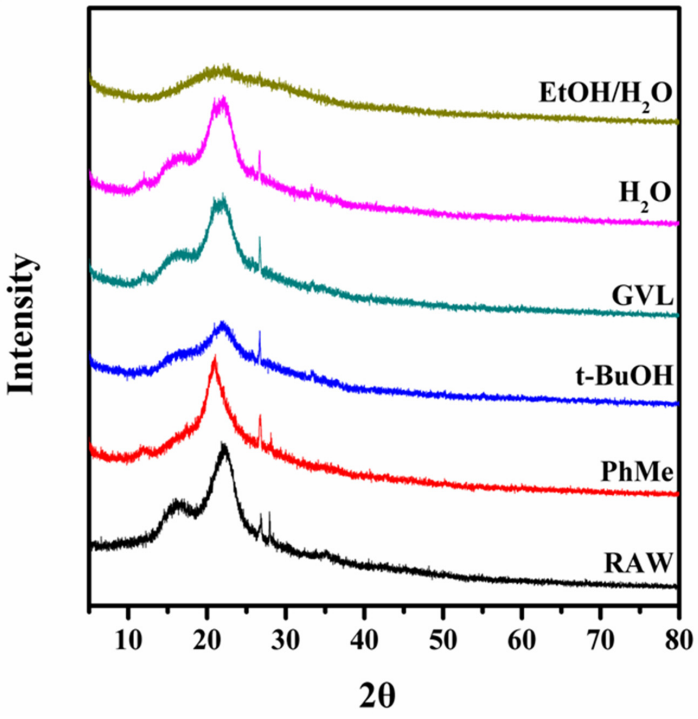


Figure 8. XRD analysis of lignocellulose and the cellulose-enriched fraction in different solvents.

It is also worth discussing the possible transition from cellulose I to cellulose III_I. As reported in the literature [33], this transformation is typically accompanied by a shift in the (002) reflection from a 2θ value of about 23° to approximately 21° when cellulose I is converted to cellulose III_I. In the present work, the lignocellulose obtained after treatment with the pressurized ammonia/PhMe system appeared to contain cellulose III_I with relatively high crystallinity, as reflected by a narrow and intense (002) peak. This feature seems to suggest that the pressurized ammonia/PhMe system may have promoted a more ordered crystalline arrangement, or possibly induced a partial crystal transition, rather than simply causing amorphization. Such an observation may also help explain why the raw lignocellulose treated with the pressurized ammonia/PhMe system still exhibited distinct diffraction peaks, in contrast to the other samples.

In contrast, the lignocellulose treated by the pressurized ammonia/50 vol% ethanol aqueous solution system displayed weaker and less distinct characteristic diffraction peaks, and its peak profile appeared similar to the typical pattern of amorphous cellulose reported in the literature [33]. These observations seem to indicate that the composite solvent system may effectively reduce the crystallinity of cellulose and partially disrupt the dense cross-linked network of lignocellulose, thereby facilitating deep lignocellulose fractionation. Such a trend is highly consistent with the SEM morphological observations and component quantification results.

Nevertheless, it should be acknowledged that the present XRD results only provide qualitative structural variation trends rather than accurate quantitative crystallinity changes. Reliable determination of the crystallinity index, peak deconvolution fitting, and quantitative uncertainty analysis requires standardized algorithms and repeated parallel measurements. These contents are beyond the scope of the current work and will be systematically investigated in future studies to support more quantitative structural eValuation.

3.3.3. Elemental Analysis

Elemental analysis was performed to determine the nitrogen content of the fractionated components obtained from lignocellulose fractionation in the pressurized ammonia/50 vol% ethanol aqueous solution system, and the detailed results are listed in Table 2. The nitrogen contents of raw lignocellulose, the cellulose-enriched fraction, and hemicellulose-enriched acetone-insoluble fraction remained at very low levels. In contrast, the isolated lignin-enriched acetone extract fraction exhibited a remarkable rise in nitrogen content. Although a simple concentration of inherent biomass nitrogen, adsorbed ammonia or ammonium salts cannot fully account for such substantial nitrogen elevation, these results imply that nitrogen-containing species from ammonia tend to accumulate in the lignin fraction. Supported by the relevant literature [34,35], ammonia may react with lignin fragments under ammonolysis conditions to form chemically bound nitrogen-containing products. This observation suggests the preferential incorporation of nitrogen species into lignin rather than cellulose and hemicellulose, facilitating the selective modification and efficient fractionation of lignocellulose components.

Table 2. Elemental analysis of lignocellulose and each component after fractionation.

No.	Component	C (%)	H (%)	N (%)
1	Raw lignocellulose	41.64	5.082	0.85
2	Cellulose-enriched fraction (8 MPa NH_3/H_2O)	37.50	5.196	0.59
3	Cellulose-enriched fraction (8 MPa $NH_3/EtOH/H_2O$)	38.04	5.339	0.49
4	Hemicellulose-enriched acetone-insoluble fraction (8 MPa $NH_3/EtOH/H_2O$)	43.59	5.852	0.67
5	Lignin-enriched acetone extract fraction (8 MPa $NH_3/EtOH/H_2O$)	44.12	5.586	4.61

3.3.4. XPS Analysis

The high-resolution N 1s spectrum was deconvoluted into two main components, as shown in Figure 9. The peak centered at 399.1 eV is assigned to covalently bonded amine species (C–N) formed between ammonia and lignin fragments. The peak at 401.5 eV corresponds to protonated ammonium or hydrogen-bonded adsorbed ammonia, which interacts with the lignin surface without covalent C–N linkages. This result demonstrates that both covalently bound nitrogen and adsorbed nitrogen coexist in the lignin-enriched acetone extract fraction [36–38].

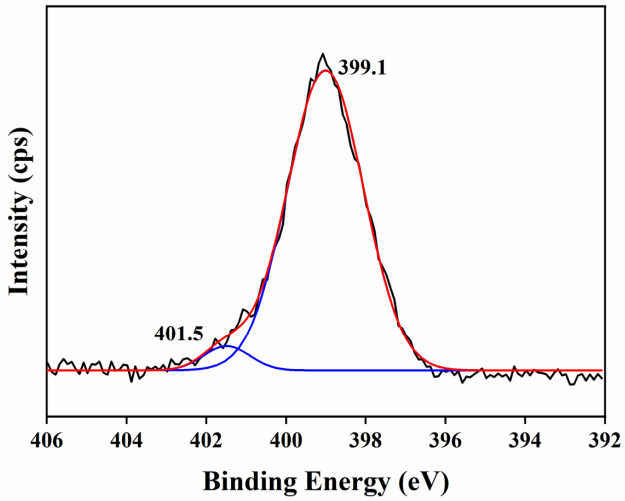


Figure 9. High-resolution N 1s XPS spectrum of lignin-enriched acetone extract fraction (8 MPa NH_3/EtOH/H_2O). The black line represents the experimental N 1s spectrum, the red line is the total fitted curve, and the blue lines correspond to the deconvoluted N-containing species.

3.4. Lignocellulose Fractionation Mechanism

Combined with the above single-factor process experiments, SEM morphological observations, XRD crystal structure tests, elemental analysis and N 1s XPS spectra, a hypothetical fractionation pathway of corn straw lignocellulose in the pressurized ammonia/50 vol% ethanol aqueous solution system is proposed, as illustrated in Figure 10. Natural lignocellulose possesses a dense cross-linked network constructed by cellulose, hemicellulose, and lignin. Cellulose forms a stable cellulose I crystal skeleton, while hemicellulose and lignin encapsulate the cellulose surface via hydrogen bonds and covalent bonds, forming physical barriers and structural constraints, which is the key reason for the difficult dissociation of lignocellulose.

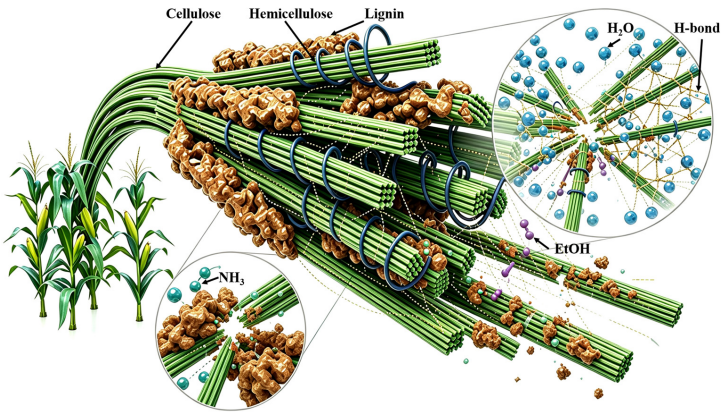


Figure 10. A hypothetical fractionation mechanism of lignocellulose in pressurized ammonia with 50 vol% ethanol aqueous solution system.

Under the preferable process conditions (200 °C, 8 MPa, 6 h, 50 vol% ethanol aqueous solution), the composite solvent and pressurized ammonia system produce a significant fractionation effect. First, the ethanol–water mixed solvent has both polarity and permeability. Water molecules can efficiently disrupt the intermolecular hydrogen bonds of lignocellulose and loosen the dense stacked structure. Small ethanol molecules penetrate cellulose microcrystalline regions, weaken the hydrogen-bond network within cellulose crystalline domains, and reduce cellulose crystallinity, which is consistent with the XRD results showing decreased diffraction intensity, reduced crystallite size and partial structural disorder under the preferable conditions. Second, the mixed solvent can selectively dissolve and remove amorphous hemicellulose, break the filling and cross-linking structure on the fiber surface, and fully expose the internal cellulose skeleton.

Meanwhile, the pressurized ammonia system participates in the selective thermochemical transformation of lignin. Elemental analysis shows that ammonia-derived nitrogen is preferentially enriched in lignin-rich fractions. The deconvolution of N 1s spectra confirms the presence of covalently bound nitrogen species, supporting the interaction between ammonia and lignin fragments. The active nitrogen-containing species in the system exert negligible modification effects on the stable crystal structure of cellulose and hemicellulose, and may facilitate the structural disruption of lignin macromolecules. Such ammonia-mediated thermochemical treatment promotes the fragmentation of lignin macromolecules under elevated temperature and pressure, consistent with the published literature [28,29,39]. It should be noted that the precise identification of cleaved lignin linkages (e.g., C–O and C–C bonds) requires advanced characterization techniques such as 2D HSQC NMR, which were not performed in the present study and will be explored in future work. This potential deconstruction tendency may enhance the solvent solubility of lignin and facilitate its efficient removal from the fiber skeleton. Nonpolar and weakly polar solvents fail to effectively disrupt the lignocellulose cross-linked structure due to insufficient penetration and dissolution capacity, resulting in only minor fiber damage. Single water or ethanol solvent systems lack this ammonia-mediated thermochemical effect and exhibit limited lignin removal efficiency, thereby delivering inferior fractionation performance compared with the composite system.

In summary, the combined effects of solvent infiltration, crystalline structure disruption, hemicellulose dissolution, and potential ammonia-promoted lignin deconstruction collectively contribute to the superior fractionation performance of the composite system. This integrated strategy enables efficient and selective removal of hemicellulose and lignin while retaining high-purity cellulose skeletons, thereby achieving deep and targeted lignocellulose fractionation. The proposed mechanism is fully consistent with the results of compositional analysis, elemental analysis, XPS, microscopic morphology, and crystalline structure characterization.

4. Conclusions

In this study, a pressurized ammonia/ethanol–water mixed system was developed for the fractionation of corn straw lignocellulose. Through exploratory single-factor screening, a set of preferable operating parameters was identified within the tested ranges: 0.4 g lignocellulose dosage, 20 mL of 50 vol% ethanol aqueous solution, 200 °C, 6 h, and 8 MPa. Under these conditions, the cellulose-enriched fraction exhibited a cellulose purity of 89.6 ± 1.4% and a cellulose recovery of 85.0 ± 2.1%. The observed fractionation performance is presumably attributable to a combined mechanism. The ethanol–water cosolvent is hypothesized to weaken the hydrogen-bond networks within the lignocellulosic matrix, thereby improving its susceptibility to chemical attack. Preferential nitrogen enrichment in lignin-rich fractions confirms ammonia-triggered thermochemical reactions. XPS N 1s

results further verify covalent C–N bond formation between ammonia and lignin fragments; such interactions may trigger potential lignin deconstruction via possible C–O and C–C bond cleavage, facilitating lignin removal while retaining cellulose skeletons. These preliminary results suggest that the proposed system provides a promising selective strategy for lignocellulose valorization. Future work will focus on mechanistic validation of the proposed lignin-modification and bond-cleavage pathways, together with further optimization of operating conditions.

Supplementary Materials: The following supporting information can be downloaded at: https://www.mdpi.com/article/10.3390/chemistry8100136/s1, Table S1. Raw numerical data for Figures 2–6.

Author Contributions: Conceptualization, Y.L.; methodology, Y.L., Y.H., B.W. and S.D.; resources, Y.L., X.Z. and Y.Y.; writing—original draft preparation, Y.L.; writing—review and editing, Y.L. and B.R.; supervision, Y.L. and X.Y. All authors have read and agreed to the published version of the manuscript.

Funding: This research was funded by the financial support from Science and Technology Development Plan Project of Jilin Province, China, grant number YDZJ202201ZYTS363.

Data Availability Statement: The original contributions proposed in this study are included in the article. Further inquiries can be sent directly to the corresponding author.

Acknowledgments: Generative AI (ByteDance Seed large language model) was used to assist drafting the graphical abstract. All scientific frameworks, structural layouts and annotations were designed, revised and verified by the authors to ensure consistency with the experimental results and scientific accuracy of this work.

Conflicts of Interest: The authors declare no conflicts of interest.

References

1. Zhou, M.; Tian, X.J. Development of different pretreatments and related technologies for efficient biomass conversion of lignocellulose. *Int. J. Biol. Macromol.* **2022**, *202*, 256–268. [CrossRef]
2. Zhang, R.; Gao, H.R.; Wang, Y.T.; He, B.Y.; Lu, J.; Zhu, W.B.; Peng, L.C.; Wang, Y.T. Challenges and perspectives of green-like lignocellulose pretreatments selectable for low-cost biofuels and high-value bioproduction. *Bioresour. Technol.* **2023**, *369*, 128315. [CrossRef]
3. Sulis, D.B.; Lavoine, N.; Sederoff, H.; Jiang, X.; Marques, B.M.; Lan, K.; Cofre-Vega, C.; Barrangou, R.; Wang, J.P. Advances in lignocellulosic feedstocks for bioenergy and bioproducts. *Nat. Commun.* **2025**, *16*, 1244. [CrossRef]
4. Zhao, L.; Sun, Z.F.; Zhang, C.C.; Nan, J.; Ren, N.Q.; Lee, D.J.; Chen, C. Advances in pretreatment of lignocellulosic biomass for bioenergy production: Challenges and perspectives. *Bioresour. Technol.* **2022**, *343*, 126123. [CrossRef]
5. Himmel, M.E.; Ding, S.Y.; Johnson, D.K.; Adney, W.S.; Nimlos, M.R.; Brady, J.W.; Foust, T.D. Biomass recalcitrance: Engineering plants and enzymes for biofuels production. *Science* **2007**, *315*, 804–807. [CrossRef]
6. Zoghlami, A.; Paës, G. Lignocellulosic Biomass: Understanding Recalcitrance and Predicting Hydrolysis. *Front. Chem.* **2019**, *7*, 874. [CrossRef]
7. Tessera, G.M.; Abera, M.K.; Habtu, N.G.; Misganaw, F.W. Advances in electromagnetic radiation-assisted pretreatment of lignocellulosic biomass as a green method: A review. *Biomass Convers. Biorefin.* **2025**, *15*, 13165–13189. [CrossRef]
8. St'Ana, D.B.; Kelbert, M.; de Araújo, P.H.H.; de Andrade, C.J. Physical Pretreatments of Lignocellulosic Biomass for Fermentable Sugar Production. *Sustain. Chem.* **2025**, *6*, 13. [CrossRef]
9. Barba, F.J.; Brianceau, S.; Turk, M.; Boussetta, N.; Vorobiev, E. Effect of Alternative Physical Treatments (Ultrasounds, Pulsed Electric Fields, and High-Voltage Electrical Discharges) on Selective Recovery of Bio-compounds from Fermented Grape Pomace. *Food Bioprocess Technol.* **2015**, *8*, 1139–1148. [CrossRef]
10. Zhang, X.Y.; Liu, A.; Li, X.H.; Xu, W.B.; Duan, X.X.; Shi, J.Y.; Li, X.Y. Research progress of deep eutectic solvents in lignocellulosic biomass pretreatment. *Cellulose* **2025**, *32*, 4637–4650. [CrossRef]
11. Kim, J.S.; Lee, Y.Y.; Kim, T.H. A review on alkaline pretreatment technology for bioconversion of lignocellulosic biomass. *Bioresour. Technol.* **2016**, *199*, 42–48. [CrossRef]
12. Deng, W.P.; Feng, Y.C.; Fu, J.; Guo, H.W.; Guo, Y.; Han, B.X.; Jiang, Z.C.; Kong, L.Z.; Li, C.Z.; Liu, H.C.; et al. Catalytic conversion of lignocellulosic biomass into chemicals and fuels. *Green Energy Environ.* **2023**, *8*, 10–114. [CrossRef]

13. Wozniak, A.; Kuligowski, K.; Swierczek, L.; Cenian, A. Review of Lignocellulosic Biomass Pretreatment Using Physical, Thermal and Chemical Methods for Higher Yields in Bioethanol Production. *Sustainability* **2025**, *17*, 287. [CrossRef]
14. Khan, M.A.; Dharmalingam, B.; Chuetor, S.; Cheng, Y.S.; Sriariyanun, M. Comprehensive review on effective conversion of lignocellulosic biomass to levulinic acid. *Biomass Convers. Biorefin.* **2025**, *15*, 29681–29696. [CrossRef]
15. Anu, R.C.; Alokika, A.; Kuhad, R.C.; Rapoport, A.; Kumar, V.; Singh, D.; Kumar, V.; Tiwari, S.K.; Ahlawat, S.; Singh, B. Biological pretreatment of lignocellulosic biomass: An environment-benign and sustainable approach for conversion of solid waste into value-added products. *Crit. Rev. Environ. Sci. Technol.* **2024**, *54*, 771–796. [CrossRef]
16. Tiwari, A.; Chen, C.W.; Haldar, D.; Patel, A.K.; Dong, C.D.; Singhania, R.R. Laccase in Biorefinery of Lignocellulosic Biomass. *Appl. Sci.* **2023**, *13*, 4673. [CrossRef]
17. Baksi, S.; Saha, D.; Saha, S.; Sarkar, U.; Basu, D.; Kuniyal, J.C. Pre-treatment of lignocellulosic biomass: Review of various physico-chemical and biological methods influencing the extent of biomass fractionation. *Int. J. Environ. Sci. Technol.* **2023**, *20*, 13895–13922. [CrossRef]
18. Ledakowicz, S. Biochemical Processes of Lignocellulosic Biomass Conversion. *Energies* **2025**, *18*, 3353. [CrossRef]
19. Li, X.L.; Shi, Y.; Kong, W.W.; Wei, J.P.; Song, W.J.; Wang, S.Y. Improving enzymatic hydrolysis of lignocellulosic biomass by bio-coordinated physicochemical pretreatment-A review. *Energy Rep.* **2022**, *8*, 696–709. [CrossRef]
20. Pereira, N., Jr. Biochemical Conversion of Lignocellulosic Biomass in Biorefinery Systems. *Fermentation* **2026**, *12*, 88. [CrossRef]
21. Shirkavand, E.; Baroutian, S.; Gapes, D.J.; Young, B.R. Combination of fungal and physicochemical processes for lignocellulosic biomass pretreatment—A review. *Renew. Sustain. Energy Rev.* **2016**, *54*, 217–234. [CrossRef]
22. Torres, R.S.; Bustamante, E.O.; Flores, A.C.E.; Guzmán, R.G.R. Physico-chemical and electrochemical delignification as a pretreatment of lignocellulosic biomass for different applications: A mini-review. *Cellul. Chem. Technol.* **2024**, *58*, 737–746. [CrossRef]
23. Wang, J.B.; Zhang, C.; Shao, Y.; Xie, F.; Yang, R.L.; Luo, H.Z. Recent advances in amine-based pretreatment for the degradation of lignocellulosic biomass and its application in microbial fermentation for chemical production. *Bioprocess Biosyst. Eng.* **2026**, *49*, 759–775. [CrossRef]
24. Zhao, C.; Shao, Q.; Chundawat, S.P.S. Recent advances on ammonia-based pretreatments of lignocellulosic biomass. *Bioresour. Technol.* **2020**, *298*, 122446. [CrossRef]
25. Chai, Y.H.; Yusup, S.; Kadir, W.N.A.; Wong, C.Y.; Rosli, S.S.; Ruslan, M.S.H.; Chin, B.L.F.; Yiin, C.L. Valorization of Tropical Biomass Waste by Supercritical Fluid Extraction Technology. *Sustainability* **2021**, *13*, 233. [CrossRef]
26. Escobar, E.; Silva, T.; Pirich, C.; Corazza, M.; Pereira Ramos, L. Supercritical Fluids: A Promising Technique for Biomass Pretreatment and Fractionation. *Front. Bioeng. Biotech.* **2020**, *8*, 252. [CrossRef]
27. Oro, C.E.D.; Mulinari, J.; de Oliveira, C.R.S.; da Silva, A.H., Jr.; Rodrigues, É.; Dallago, R.M.; Tres, M.V. Recent Advances in Subcritical Water Pretreatment of Lignocellulosic Biomass: Integrating Modern Extraction Techniques for Biorefinery Applications. *Bioenergy Res.* **2025**, *18*, 99. [CrossRef]
28. Zhang, Y.D.; Zhang, X.H.; Chi, S.S.; Li, Z.Q. Pulping of Bamboo using Supercritical Ammonia with Recovery and Reuse of the Ammonia. *Bioresources* **2019**, *14*, 5586–5594. [CrossRef]
29. Bludworth, J.; Knopf, F.C. Reactive extraction of lignin from wood using supercritical ammonia-water mixtures. *J. Supercrit. Fluids* **1993**, *6*, 249–254. [CrossRef]
30. Sluiter, A.; Hames, B.; Ruiz, R.; Scarlata, C.; Sluiter, J.; Templeton, D.; Crocker, D. *Determination of Structural Carbohydrates and Lignin in Biomass; NREL Laboratory Analytical Procedure (LAP)*; Technical Report NREL/TP-510-42618; National Renewable Energy Laboratory: Golden, CO, USA, 2011.
31. Segal, L.; Creely, J.J.; Martin, J.A.; Conrad, C.M. An empirical method for estimating the degree of crystallinity of native cellulose using the X-ray diffractometer. *Text. Res. J.* **1959**, *29*, 786–794. [CrossRef]
32. Sánchez, P.B.; Tsubaki, S.; Pádua, A.A.H.; Wada, Y. Kinetic analysis of microwave-enhanced cellulose dissolution in ionic solvents. *Phys. Chem. Chem. Phys.* **2020**, *22*, 1003–1010. [CrossRef]
33. Mittal, A.; Katahira, R.; Himmel, M.E.; Johnson, D.K. Effects of Alkaline or Liquid-Ammonia Treatment on Crystalline Cellulose: Changes in Crystalline Structure and Effects on Enzymatic Digestibility. *Biotechnol. Biofuels* **2011**, *4*, 41. [CrossRef]
34. Yoo, C.G.; Kim, H.; Lu, F.; Azarpira, A.; Pan, X.; Oh, K.K.; Kim, J.S.; Ralph, J.; Kim, T.H. Understanding the Physicochemical Characteristics and the Improved Enzymatic Saccharification of Corn Stover Pretreated with Aqueous and Gaseous Ammonia. *Bioenergy Res.* **2015**, *9*, 67–76. [CrossRef]
35. Prinsen, P.; Narani, A.; Rothenberg, G. Lignin Depolymerisation and Lignocellulose Fractionation by Solvated Electrons in Liquid Ammonia. *ChemSusChem* **2017**, *10*, 1022–1032. [CrossRef]
36. Zheng, Q.; Nong, G.; Li, N. Preparation and Structural Analysis of a Water-Soluble Aminated Lignin. *Polymer* **2024**, *16*, 1237. [CrossRef]
37. Zhang, Y.; Liu, Q.; Ma, W.; Liu, H.; Zhu, J.; Wang, L.; Pei, H.; Liu, Q.; Yao, J. Insight into the synergistic adsorption-reduction character of chromium(VI) onto poly(pyrogallol-tetraethylene pentamine) microsphere in synthetic wastewater. *J. Colloid Interface Sci.* **2022**, *609*, 825–837. [CrossRef]

38. Shang, Y.; Zhu, G.; Yan, D.; Liu, Q.; Gao, T.; Zhou, G. Tannin cross-linked polyethyleneimine for highly efficient removal of hexavalent chromium. *J. Taiwan Inst. Chem. Eng.* **2021**, *119*, 52–59. [CrossRef]
39. Xu, L.; Zhang, S.J.; Zhong, C.; Li, B.Z.; Yuan, Y.J. Alkali-Based Pretreatment-Facilitated Lignin Valorization: A Review. *Ind. Eng. Chem. Res.* **2020**, *59*, 16923–16938. [CrossRef]

Disclaimer/Publisher's Note: The statements, opinions and data contained in all publications are solely those of the individual author(s) and contributor(s) and not of MDPI and/or the editor(s). MDPI and/or the editor(s) disclaim responsibility for any injury to people or property resulting from any ideas, methods, instructions or products referred to in the content.